

Structural Design and Frequency Tuning of Piezoelectric Energy Harvesters Based on Topology Optimization

Abbas HOMAYOUNI-AMLASHI¹, Micky RAKOTONDRABE², *member, IEEE* and Abdenbi MOHAND-OUSAI¹

Abstract—Vibrational piezoelectric energy harvesters (vPEH) are of great interest in several fields such as autonomous sensors and wireless sensor networks, bird tracking devices, or autonomous miniaturized robotic systems. They capture energy from mechanical vibrations available in the ambient environment and convert it into electrical one to power those systems. Basically, a vPEH is composed of three main parts: the transducer mechanical structure, an electronic interface and the storage unit. In this paper, we focus on the optimization of the mechanical structure of the harvester. To this end, an optimization framework based on topology optimization is proposed. It consists to combine the Solid Isotropic Material with Penalization (SIMP) approach and frequency tuning technique to further increase the efficiency of the harvesters. The fundamental frequency of the design is tuned by considering the mass of the attachment as an optimization variable in addition to the classical density and polarity variables. Two numerical examples, including a new piezoelectric energy harvester configuration, are investigated to demonstrate the effectiveness of the topology optimization framework.

I. INTRODUCTION

Motivated by environmental issues, energy harvesting (EH) as a power supply alternative has been given much attention in the last decades. Solar, thermal and kinetic energies are the most abundant and accessible forms of energies in the environment. Within kinetic energy sources, vibrations are of particular interest as they are ubiquitous: in cars, from walking person, from appliances with motors and from animal movements. To harvest energy from vibrations, vibrational piezoelectric energy harvester (vPEH) can be used. Its principle is to convert the energy generated by oscillating deformation of a piezoelectric transducer into electricity thanks to piezoelectric direct effect [1]. This allows for replacing the classical power supplies such as batteries which have a short lifespan and considerable cost of maintenance with renewable ones. In fact, vPEHs are highly efficient at small-scale applications like microelectromechanical systems [2], wireless sensor networks [3], bird tracking devices [4] or autonomous robotic systems [5]. Meanwhile, these applications generally raise restrictions and constraints

that should be respected when designing efficient and appropriate harvesters. Some examples are volume and weight limitation. Hence, researchers proposed different optimization techniques to design vPEH, specifically to maximize the electrical output for the given mechanical input under these constraints [6]. Considering only the mechanical structure of the vPEH, these design strategies can be classified into two major categories: form optimization (which includes particular topology optimization) and frequency tuning.

Topology optimization is a mathematical approach based on material distribution [7]. Basically, it allows to find an optimal layout in a design domain while respecting a certain specification and attaining desired performance of the structure. This powerful design tool, in particular SIMP (Solid Isotropic with Material Penalization) method [8], was initially proposed to solve compliance problems dealing with light-weight structures [9], but was later extended to multi-physics problems including piezoelectricity. Rupp et al [10], [11] applied for the first time topology optimization for vPEH while electrical circuit coupling was also considered in the modeling. Zheng et al [12] performed static topology optimization for vPEH. Noh et al. [13] extended the work of Zheng [12] to topology optimization of vPEH under dynamic load. Following these works and inspired by [14], Salas [15] employed the innovative extension of SIMP called PEMAP-P to optimize the polarization profile of the vPEH in addition to its density layout. Most recently, we applied topology optimization to design actuators [16]–[18] and vPEH under external in-plane force considering different boundary conditions [19], [20] and multi-directional vPEH [21]. In addition to the theoretical aspects, experimental investigations were carried out to demonstrate the vPEH efficiency. Motivated by these achievements, we developed 2D topology optimization MATLAB codes for piezoelectric energy harvesters [22].

On the other hand, the best efficiency of a vPEH can be obtained when it is excited at its resonance frequency. Frequency matching is therefore very crucial for every PEH since only 2% deviation of resonance frequency from excitation frequency will drop the electrical output power by 50% [23]. Moreover, the available excitation frequency in real applications is generally between 10 to 30 Hz [1], which is below the normal resonance frequency of the vPEHs. The classical and conventional method to match the resonance frequency with the low excitation frequency is to attach a lumped mass at the tip of the cantilever PEH [24]. Several researchers considered the modification of eigenfrequencies [25] and eigenmodes [26] in vPEH by topology optimization to improve the electromechanical coupling coefficient. Al-

¹ Université de Franche-Comté, SUPMICROTECH, CNRS, institut FEMTO-ST, F-25000 Besançon, France .

²LGP laboratory, National School of Engineering in Tarbes (ENIT-INPT), University of Toulouse, Tarbes - France.

Contacts: abdenbi.mohand@femto-st.fr
mrakoton@enit.fr.

This work was supported by MultiOptim Chrysalide emergent project (UFC) and Robocap project. It was also partially supported by the national CODE-TRACK project (ANR-17-CE05-0014-01), the Bourgogne Franche-Comté region CONAFLU project and ANR OptoBot project.

though these complementary approaches optimize the layout of the vPEH, there is no work that considers the lumped mass inside the topology optimization.

In this work, we suggest combining topology optimization and frequency tuning to raise further the efficiency of vPEH. The idea consists to consider the planar excitation in the topology optimization while defining a constraint for the fundamental frequency which is related to the out-of-plane bending deformation. To tackle the challenges of eigenfrequency within topology optimization approach, we define the vPEH attachment's mass as a new optimization variable in addition to the density and the polarity. Aiming for low weight piezoelectric energy harvester, a new configuration is proposed to minimize the fundamental resonance frequency and the mass of the attachment simultaneously. Based on the bi-morph structure this configuration is able to harvest energy from multi-directions. The performance of the optimization algorithm in terms of matching the resonance frequency to the desired one is assessed by simulation. The obtained results in MATLAB and COMSOL Multiphysics demonstrated that the algorithm successfully restricted the fundamental frequency close to the desired one while respecting mass and volume constraints of the vPEH.

II. PIEZOELECTRIC ENERGY HARVESTER

A. Vibrational piezoelectric harvester

Generally, piezoelectric materials can convert mechanical to electrical energy without any additional structure which makes them highly favorable in applications where vibrations are abundant. However, the amount of harvested energy by the vPEH remains low. Overcoming this limitation by employing topology optimization and frequency tuning approaches is challenging but would increase further the vPEH efficiency. This will be made possible by considering the physics of the piezoelectric material within the optimization problem. It is worth noticing that only the mechanical structure of the vPEH is optimized here. The piezoelectric material itself, the fabrication process and the electronic circuit of the vPEH could be also optimized as it is suggested in the literature, but all of these aspects are out of the scope of this study. To apply the topology optimization it is necessary to provide the finite element model of the system which will be discussed next.

B. Finite element modeling of piezoelectric material

A bi-morph piezoelectric plate model is the most efficient form of vPEH in the meso scale [27] which is chosen to be optimized. As illustrated in Fig. 1, it consists of two piezoelectric layers sandwiched between three electrodes: on top, middle and bottom electrode.

The polarization axis for the piezoelectric materials is parallel to the z direction of the coordinate system while the direction will be determined later by optimization. From mathematical point of view, all the necessary steps to derive the finite element model of the bi-morph plate including (i) piezoelectric material modeling, (ii) discretization, (iii) derivation of elemental stiffness matrices (iv) and assembly

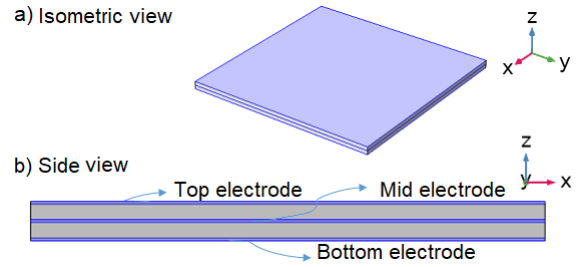


Fig. 1. Bi-morph piezoelectric plate.

of the global matrices are already established and readers can refer to our previous works for more details [21].

The global finite element equilibrium equation for a multi-layer piezoelectric plate can be expressed as follows:

$$\begin{bmatrix} M & 0 \\ 0 & 0 \end{bmatrix} \begin{bmatrix} \ddot{U} \\ \ddot{\Phi} \end{bmatrix} + \begin{bmatrix} K_{uu} & K_{u\phi} \\ K_{\phi u} & -K_{\phi\phi} \end{bmatrix} \begin{bmatrix} U \\ \Phi \end{bmatrix} = \begin{bmatrix} F \\ Q \end{bmatrix} \quad (1)$$

where U and ϕ are the vectors of the mechanical displacement and electric potential respectively. F and Q are the applied external mechanical force and electrical charge. M , K_{uu} , $K_{u\phi}$, $K_{\phi\phi}$ are the global mass matrix, mechanical stiffness matrix, piezoelectric coupling matrix and piezoelectric permittivity matrix respectively. The global matrices are formed by assembling the elemental matrices [22]. The global equilibrium equation (1) can be normalized to avoid the numerical instabilities and can be re-written based on the normalization which is provided in Ref. [22] as

$$\begin{bmatrix} \tilde{K}_{uu} - \tilde{M}\tilde{\Omega}^2 & \tilde{K}_{u\phi}B \\ B^T\tilde{K}_{u\phi}^T & -\gamma B^T\tilde{K}_{\phi\phi}B \end{bmatrix} \begin{bmatrix} \tilde{U} \\ V_p \end{bmatrix} = \begin{bmatrix} \tilde{F} \\ 0 \end{bmatrix} \quad (2)$$

in which, $(\tilde{\cdot})$ stands for the normalized quantities. B is a Boolean matrix to apply the equipotential condition on the electrodes with dimension $N_e \times N_p$ where N_e is the number of nodes and N_p is the number of potential electrodes where in our case $N_p = 2$. $\tilde{\Omega}$ is the normalized excitation frequency, V_p is the generated voltage by the vPEH and γ is the normalized factor that keeps the solution of the system equal before and after applying the normalization.

In general, the target is to excite a vPEH at its resonance frequency to harvest the maximum possible amount of energy. Therefore, in addition to what has been mentioned in our previous works [21], [22], the resonance frequency will be calculated through the finite element approach. The resonance frequency is the natural frequency of the system at short circuit condition. At open circuit condition, the natural frequencies of the system are the anti-resonance frequency [28]. Therefore the fundamental resonance frequency at $V_p = 0$ can be calculated,

$$[\tilde{K}_{uu} - \tilde{M}\tilde{\omega}_s^2] \Psi_s = 0 \quad (3)$$

in which $\tilde{\omega}_s$ is the natural frequency at short circuit condition and Ψ_s is the related eigenvector. Now, based on the built FEM of the piezoelectric plate and the provided resonance equation, topology optimization algorithm can be applied to maximize

the harvested energy of the bi-morph vPEH by optimizing the topology and modifying the resonance frequency.

III. TOPOLOGY OPTIMIZATION OF vPEH

In addition to the topology optimization framework proposed in [21], there are aspects that are new in this study including new vPEH configuration and tuning the resonance frequency. To apply the topology optimization for the desired vPEH system, the optimization problem should be defined primarily. In this regard, we have to define the objective function, constraints and optimization variables. These will be discussed in the upcoming subsections.

A. Objective function

For the definition of objective function, the weighted sum of the stored mechanical and electrical energy of the vPEH is considered:

$$J = w_j \Pi^S - (1 - w_j) \Pi^E \quad (4)$$

where w_j is the weighing factor and the energies that can be expressed as:

$$\begin{aligned} \Pi^S &= \left(\frac{1}{2}\right) \tilde{U}^T \overline{K_{uu}} \tilde{U}, \quad \Pi^E = \left(\frac{1}{2}\right) V_p^T \overline{K_{\phi\phi}} V_p \\ \overline{K_{uu}} &= [\tilde{K}_{uu} - \tilde{M} \tilde{Q}^2]_{bc}, \quad \overline{K_{\phi\phi}} = \gamma B^T \tilde{K}_{\phi\phi} B \end{aligned} \quad (5)$$

where $([\]_{bc})$ shows the application of mechanical boundary conditions. This defined objective function aims for increasing the efficiency of the vPEH by maximization of electrical energy while minimizing the stored mechanical energy (deformation) to assure the static stability of the system.

B. Tuning the resonance frequency

To tune the resonance frequency a constraint should be defined on the fundamental natural frequency of the system. Concretely, a lumped mass is associated to the tip of the vPEH and considered as a new optimization variable for the topology optimization of the vPEH. This helps tuning the natural frequency of the structure in the scale of the excitation in real applications and also to produce inertia force which induces strain in the vPEH. The lumped mass modifies the mass matrix of the system as follows,

$$\tilde{M} = \sum_{i=1}^{NE} \tilde{m}_i + y [\tilde{M}_{mass}] \quad (0 \leq y \leq 1) \quad (6)$$

in which \tilde{m}_i is the elemental mass, i is the element number and y is the optimization variable that stands for the ratio of maximum possible mass of the attachment. By definition of y here, we give more freedom to the optimization in terms of convergence to a perfect solid void material in the final layout. The reason is that the variable y can increase or decrease the total mass of the vPEH without changing its stiffness. This optimization variable helps optimization solver to converge to a fully black and white final layout and to avoid the greyness problem which is a common problem in topology optimization with frequency tuning [29].

C. Optimization variables

To specify other optimization variables, we can refer to the material interpolation scheme for the SIMP (Solid Isotropic Material with Penalization) approach and its extension for piezoelectric materials known as Piezoelectric Material with Penalization and Polarization" (PEMAP-P) which can be expressed as follows [13], [14]:

$$\begin{aligned} \tilde{k}_{uu}(x_i) &= \left[\frac{x_{min} - x_{min}^{P_{uu}}}{1 - x_{min}^{P_{uu}}} (1 - x_i^{P_{uu}}) + x_i^{P_{uu}} \right] \tilde{k}_{uu}, \\ \tilde{k}_{u\phi}(x, P) &= x^{P_{u\phi}} (2P - 1)^{PP} \tilde{k}_{u\phi}, \\ \tilde{k}_{\phi\phi}(x) &= x^{P_{\phi\phi}} \tilde{k}_{\phi\phi}, \\ \tilde{m}(x) &= x \tilde{m} \end{aligned} \quad (7)$$

where, \tilde{k}_{uu} , $\tilde{k}_{u\phi}$ and $\tilde{k}_{\phi\phi}$ are the corresponding elemental piezoelectric matrices from equation (2). p_{uu} , $p_{u\phi}$ and $p_{\phi\phi}$ are the stiffness, coupling and permittivity penalization coefficients. Coupling Matrix $\tilde{k}_{u\phi}(x, P)$ is a function of density (x) and polarization (P) which is penalized by factor p_P . The material interpolation scheme in equation (7) will attribute two optimization variables including the density (x) and polarization (P) to each element in the design domain. In addition, one optimization variable (y) is defined in equation (6) that is attributed to the lumped mass.

The first interpolation function defined in equation (7) for the stiffness matrix K_{uu} is defined to avoid the localized modes at the low density regions [30]. The reason is that, based on the SIMP material interpolation scheme, low density regions are highly flexible (soft) that produce very low and artificial eigenmodes. To remedy, the interpolation function for the stiffness matrix which is proposed by Huang et al. [29] is utilized that suppresses the localized modes.

D. Problem formulation for vPEH design

After establishing finite element mode, objective function, constraints and optimization variables, it is possible to define the global optimization formulation as follows:

$$\begin{aligned} & \text{minimize} && J \\ & \text{Subject to} && V(x) = \sum_{i=1}^{NE} x_i v_i \leq V \\ & && \omega_1 < \varpi, \\ & && 0 \leq x_i \leq 1, \quad 0 \leq P_i \leq 1, \quad 0 \leq y \leq 1 \end{aligned} \quad (8)$$

where x_i , P_i and y are the optimization variables. ϖ is the desired resonance frequency and J is the weighted sum of the energies as it has been defined in equation (4). V is the target volume which is a fraction of the overall volume of the design domain while v_i is the volume of each element and NE is the total number of elements. This constraint on the volume is equivalent to the constraint on the mass of the piezoelectric layers. By having the inequality constraint on the resonance frequency, the optimization is more relaxed than having equality constrained. On the other hand, the resonance frequency will finally match the excitation frequency as the structure tends to be more rigid during optimization iterations.

To solve the optimization problem in (8), we will use the gradient based solvers like Method of Moving Asymptotes (MMA) developed by Svanberg et al. [31], [32]. In this regard, we need the gradient of the objective function and constraint with respect to optimization variables which will be discussed next.

E. Sensitivity analysis

The procedure to derive the gradient of objective function and constraints with respect to optimization variables is known as sensitivity analysis. The sensitivity analysis of objective function is already developed and established in previous works by authors [21]. As such, without giving the details, the sensitivity of objective function with respect to the optimization variables are

$$\frac{\partial \Pi^S}{\partial x_i} = \left(\frac{1}{2} \tilde{u}_i^T + \lambda_{1,i}^T \right) \frac{\partial (\tilde{k}_{uu} - \tilde{m} \tilde{\Omega}^2)}{\partial x_i} \tilde{u}_i + \lambda_{1,i}^T \frac{\partial \tilde{k}_{u\phi}}{\partial x_i} \tilde{\phi}_i + \mu_{1,i}^T \frac{\partial \tilde{k}_{\phi u}}{\partial x_i} \tilde{u}_i - \mu_{1,i}^T \frac{\gamma \partial \tilde{k}_{\phi\phi}}{\partial x_i} \tilde{\phi}_i \quad (9)$$

$$\frac{\partial \Pi^E}{\partial x_i} = \frac{1}{2} \tilde{\phi}_i^T \frac{\gamma \partial \tilde{k}_{\phi\phi}}{\partial x_i} \tilde{\phi}_i - \mu_{2,i}^T \frac{\gamma \partial \tilde{k}_{\phi\phi}}{\partial x_i} \tilde{\phi}_i + \lambda_{2,i}^T \frac{\partial (\tilde{k}_{uu} - \tilde{m} \tilde{\Omega}^2)}{\partial x_i} u_i + \lambda_{2,i}^T \frac{\partial \tilde{k}_{u\phi}}{\partial x_i} \tilde{\phi}_i + \mu_{2,i}^T \frac{\partial \tilde{k}_{\phi u}}{\partial x_i} \tilde{u}_i \quad (10)$$

in which \tilde{u}_i and $\tilde{\phi}_i$ are the elemental displacement and potentials and μ and λ are the elemental adjoint vectors which are calculated by the following global coupled system

$$\begin{bmatrix} \overline{K_{uu}} & \overline{K_{u\phi}} \\ \overline{K_{\phi u}} & -\overline{K_{\phi\phi}} \end{bmatrix} \begin{bmatrix} \Lambda_1 \\ \Upsilon_1 \end{bmatrix} = \begin{bmatrix} -\overline{K_{uu}} \tilde{U} \\ 0 \end{bmatrix} \\ \begin{bmatrix} \overline{K_{uu}} & \overline{K_{u\phi}} \\ \overline{K_{\phi u}} & -\overline{K_{\phi\phi}} \end{bmatrix} \begin{bmatrix} \Lambda_2 \\ \Upsilon_2 \end{bmatrix} = \begin{bmatrix} 0 \\ -\overline{K_{\phi\phi}} V_p \end{bmatrix} \quad (11)$$

where Λ and Υ , are the global adjoint vectors. Now, the sensitivities with respect to polarization (P) is calculated as well [20], [21]

$$\frac{\partial \Pi^S}{\partial P_i} = \lambda_{1,i}^T \frac{\partial \tilde{k}_{u\phi}}{\partial P_i} \tilde{\phi}_i + \mu_{1,i}^T \frac{\partial \tilde{k}_{\phi u}}{\partial P_i} \tilde{u}_i \\ \frac{\partial \Pi^E}{\partial P_i} = \lambda_{2,i}^T \frac{\partial \tilde{k}_{u\phi}}{\partial P_i} \tilde{\phi}_i + \mu_{2,i}^T \frac{\partial \tilde{k}_{\phi u}}{\partial P_i} \tilde{u}_i \quad (12)$$

Here, in addition to density and polarization, the attachment variable (y) is also an optimization variable. Therefore, the sensitivity of energies with respect to this optimization variable should be calculated as well,

$$\frac{\partial \Pi^S}{\partial y} = \left(\frac{1}{2} \tilde{u}_i^T + \lambda_{1,i}^T \right) \frac{\partial (\tilde{M} \tilde{\Omega}^2)}{\partial y} \tilde{u}_i \\ \frac{\partial \Pi^E}{\partial y} = \lambda_{2,i}^T \frac{\partial (\tilde{M} \tilde{\Omega}^2)}{\partial y} u_i \quad (13)$$

To apply the constraint on the natural frequency, its gradient with respect to the optimization variables should be calculated.

To do so, the fundamental natural frequency of the system can be defined through the Rayleigh quotient [29],

$$\tilde{\omega}_s^2 = \frac{\Psi_s^T \tilde{K}_{uu} \Psi_s}{\Psi_s^T \tilde{M} \Psi_s} \quad (14)$$

The interpretation of first natural frequency by Rayleigh quotient will result in to more efficient sensitivity analysis. By following the procedure presented in [29], the sensitivities of the natural frequency's constraints with respect to optimization variables are

$$\frac{\partial \omega_s}{\partial x_i} = \frac{1}{2\omega_s \Psi_s^T \tilde{M} \Psi_s} \left[\Psi_s^T \left(\frac{\partial \tilde{k}_{uu}}{\partial x_i} - \tilde{\omega}_s^2 \frac{\partial \tilde{M}}{\partial x_i} \right) \Psi_s \right] \\ \frac{\partial \omega_s}{\partial y} = -\frac{\tilde{\omega}_s}{2\Psi_s^T \tilde{M} \Psi_s} \left[\Psi_s^T \frac{\partial \tilde{M}}{\partial y} \Psi_s \right] \quad (15)$$

Based on the sensitivity equations (10) and (12), the derivative of all piezoelectric matrices with respect to the design variables are required. The derivative of the stiffness matrix with respect to density can be calculated with the help of the material interpolation scheme in Equ. 7 as:

$$\frac{\partial \tilde{k}_{uu}}{\partial x} = \frac{1 - x_{min}}{1 - x_{min}^p} p_{uu} x_i^{p-1} K_{uu} \\ \frac{\partial \tilde{k}_{u\phi}}{\partial x_i} = p_{u\phi} (e_0 - e_{min}) x_i^{p_{u\phi}-1} (2P_i - 1)^{pP} \tilde{k}_{u\phi} \\ \frac{\partial \tilde{k}_{\phi u}}{\partial P_i} = 2pP (e_0 - e_{min}) (2P_i - 1)^{pP-1} x_i^{p_{u\phi}} \tilde{k}_{\phi u} \\ \frac{\partial \tilde{k}_{\phi\phi}}{\partial x_i} = p_{\phi\phi} (\varepsilon_0 - \varepsilon_{min}) x_i^{p_{\phi\phi}-1} \tilde{k}_{\phi\phi} \\ \frac{\partial \tilde{m}}{\partial x_i} = \tilde{m}_i, \quad \frac{\partial \tilde{m}}{\partial y} = \tilde{M}_{mass} \quad (16)$$

After performing the sensitivity analysis, the topology optimization can be implemented based on the same algorithm which is provided in [21], [22]. The results of the optimization will be discussed next.

IV. NUMERICAL EXAMPLES

The optimization framework developed in Sec. III integrates frequency tuning within the topology optimization method by considering the mass of attachment as a new optimization variable. Its implementation under MATLAB follows the same steps as described in [22]. To evaluate this algorithm, two numerical examples are considered while the efficiency of one of the examples is already proved over full plate in our previous study [21].

A. vPEH configurations

Figure 2 illustrates two configurations with different boundary conditions and mass attachment for multi-directional vPEH. The configuration in panel (a) of this figure is similar to the one presented in our previous work [21]. However, since there is a need to tune the resonance frequency and reduce the mass of the vPEH simultaneously, an alternative configuration

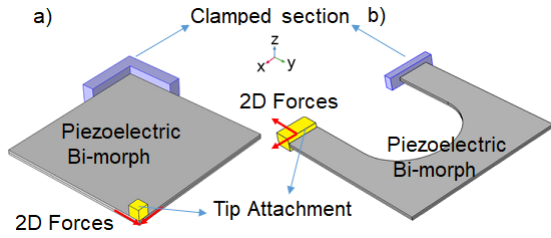


Fig. 2. Proposed configuration for multidirectional bi-morph piezoelectric energy harvesters.

is proposed in panel (b) of this figure. The main goal of this configuration is to reach the desired natural frequency with the lowest possible attached mass. The geometry and other specifications related to the optimization are mentioned in Tab. I. The penalization factors are chosen based on the strategy mentioned in [22]. The other proposition of this paper is that we considered the planar 2D forces as excitation forces of the system in TO which optimizes the structure and polarity direction of vPEH for planar excitation. On the other hand, by constraining the fundamental frequency which is related to out-of-plane bending equal to the desired excitation frequency, the harvested energy due to out-of-plane excitation will be maximized as well.

TABLE I
PARAMETERS

Parameter	Value	Parameter	Value
PZTP Thickness	0.1(mm)	ρ_{uu}	3
PZTP Length	40 (mm)	$\rho_{u\phi}$	6
PZTP Width	40 (mm)	$\rho_{\phi\phi}$	6
FEM nbr of Elements	$100 \times 100 \times 2$	ρ_p	1
Clamping Fraction	0.2	Excitation Frequency	15 Hz
Vol. Fraction	0.4	Max. Mass	1.5gr
Vibration Acc.	1g	w_j	0.1

B. Case study of bird tracking

To solve the optimization problem, the nature of the vPEH excitation in terms of frequency and acceleration should be specified according to the application. Here, we consider the case of bird tracking devices that need to be supplied by renewable energies in particular vPEH. By referring to [4], the Root Mean Square (RMS) of the body acceleration of small size birds is around 1 g in which g is the gravitational acceleration. In the same study, the reported wing beat frequency of most birds is 15 Hz. With these two important specifications, we determined the input excitation for the vPEH and the optimization as they are reported in Tab. I.

C. Optimization results

The optimization algorithm is applied to the configurations given in Fig. 2 and the resulting layouts can be seen in Fig. 3. In Fig. 3.a, the optimized layout and polarity are similar to our previous work [21] while Fig. 3.b shows the optimized layout and polarity of the proposed configuration. For simplicity, the designs in panels (a) and (b) will be called respectively design (1) and (2) in the rest of the paper.

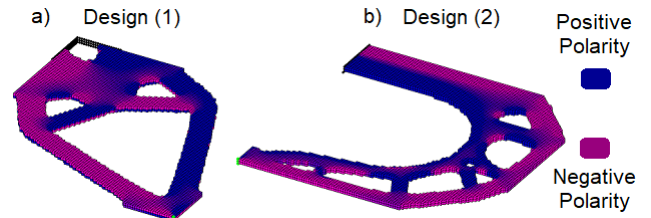


Fig. 3. Optimal layout and polarity.

Figure 4 illustrates the evolution of the numerical data during the optimization process. Several important points can be deduced from these curves. One point is that mechanical and electrical energies are more in design (2) in comparison to design (1). It means that for the same amount of input force, design (2) will produce electrical energy 5 times higher than design (1) while it has 5 times more mechanical energy as well. It can be concluded that for the same amount of excitation, design (2) may have more stress and strain than design (1). Moreover, both designs (1) and (2) satisfied the frequency constraint with 14.94 Hz and 14.84 Hz respectively. However, design (2) needs only 0.48×1.5 gr of mass while design (1) needs 0.90×1.5 gr of mass to have the fundamental resonance frequency close to 15 Hz. Thus, design (2) successfully satisfied its predetermined goal of having less amount of total weight compared to design (1). As you can see panel (d) of fig. (4), the mass of attachment start from a minimum value and increases gradually whenever the optimization needs to reduce the fundamental frequency of the design. Other important aspects such as how much stress will be produced? how much homogenized will be the harvested energy from different directions of excitation? will be answered in the FEM simulation by COMSOL Multiphysics.

D. COMSOL simulation

After transferring the optimal layouts under COMSOL, a FEM analysis is performed. As reported in Fig. 5, the natural frequencies in simulation are close (14.205 Hz and 14.54 Hz respectively) but slightly lower than the ones calculated by MATLAB. The reason may come from the cuboid elements used in MATLAB to discretize the design domain. Although a good resolution is chosen, only one element per piezoelectric layer is used. In this case, the modeled plate in MATLAB is stiffer than the modeled plate in the COMSOL Multiphysics in which more elements per thickness are used. Moreover, the eigenmodes can be seen in Fig. 5.a and Fig. 5.b. As expected, the first resonance frequency belongs to the out-of-plane bending deformation.

It is worthwhile to mention here that, to follow the optimized polarity profile as they are illustrated in Fig. 3, the method of electrode separation is utilized as it is explained in [21]. The electrode separation lines are identified in Fig. 5. It should be noted that the electrode separation line is not completely following the polarization profile due to existence of islands in optimized polarity. Readers are referred to works of Donoso et al. [33], [34] to have constraint on the electrode connectivity.

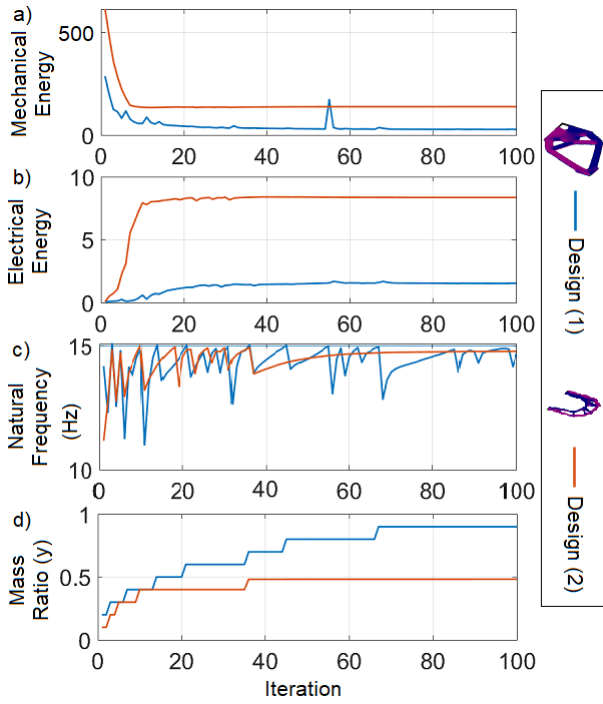


Fig. 4. MATLAB numerical results of topology optimization with constraint on the resonance frequency.

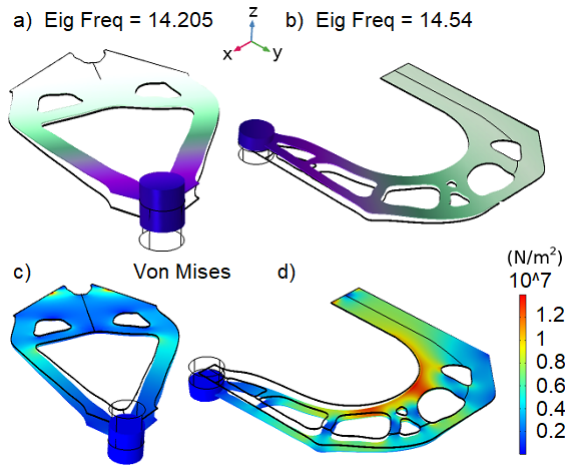


Fig. 5. a) and b) fundamental resonance frequency and mode shapes. c) and d) Von Mises stress.

The responses of the vPEHs to a multi-directional force are illustrated in Fig. 6. This force is equivalent to the inertial force on the tip mass induced by the base excitation. Similar to the results reported in Fig. 4, the electrical and mechanical energies of design (2) are higher than design (1). This means, although design (2) is providing more electrical energy, the stored mechanical energy is also higher than design (1) which is equivalent to more stress/strain in design (2). To assess this, the Von Mises stress in the designs due to an out-of-plane force that triggers the eigenmode of the design is reported in Fig. 5.c and Fig. 5.d. It is obvious that in some areas of the design (2) there are red areas which have the highest von mises stress

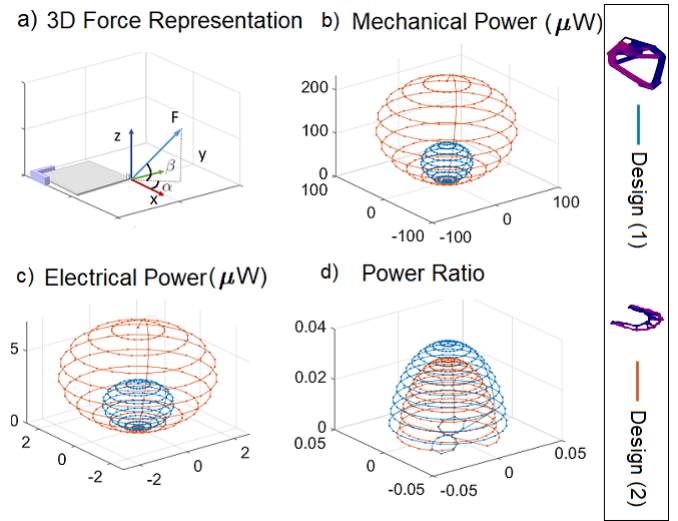


Fig. 6. COMSOL Multiphysics FEM results to investigate the performance of designs under application of 3D force. Direction of each point towards the center shows the direction of the force and the distance shows the magnitude of variable.

while with the same color spectrum, design (1) is experiencing a lower amount of stress. Thus, it is important to know when the fracture will happen especially when brittle PZTs are used. Park et al. [35] investigated this question by studying the tensile strength of PZT thin films. This study reported different ultimate tensile strengths based on the thickness of the film. For example, for $100 \mu\text{m}$ the ultimate tensile strength is reported to be 238 MPa. The ultimate stress that we are experiencing in design (2) is equal to 13 MPa which is far below the 238 MPa reported by [35]. Therefore, there will be no fracture in the piezoelectric material due to the applied excitation.

It is important to note that the geometrical dimensions of the considered vPEH in this paper can be modified to be useful for different applications. In this case, the generality of the proposed approach will remain correct.

V. CONCLUSIONS AND PERSPECTIVES

In this paper, we propose an optimization framework that combines topology optimization and frequency technique to increase the efficiency of the vPEH. To do so, the fundamental frequency of the design is tuned by considering the mass of the attachment as an optimization variable in addition to the classical density and polarity variables. A new configuration for the vPEH is proposed to lower the mass of the attachment as much as possible during the optimization while tuning the resonance frequency. The obtained results in MATLAB and COMSOL Multiphysics demonstrated that the algorithm successfully restricted the fundamental frequency close to the desired one. The efficiencies of the optimized designs are assessed in terms of satisfying the resonance frequency and the mass and volume constraints of the vPEH. Future works would concern the fabrication and the experimental characterization of the proposed configuration. It would also concern the extension of the proposed framework to design three dimensional vPEHs.

REFERENCES

- [1] H. Liu, J. Zhong, C. Lee, S.-W. Lee, and L. Lin, "A comprehensive review on piezoelectric energy harvesting technology: Materials, mechanisms, and applications," *Applied Physics Reviews*, vol. 5, no. 4, p. 041306, 2018.
- [2] W. Tian, Z. Ling, W. Yu, and J. Shi, "A review of mems scale piezoelectric energy harvester," *Applied Sciences*, vol. 8, no. 4, p. 645, 2018.
- [3] X. Tang, X. Wang, R. Cattley, F. Gu, and A. D. Ball, "Energy harvesting technologies for achieving self-powered wireless sensor networks in machine condition monitoring: A review," *Sensors*, vol. 18, no. 12, p. 4113, 2018.
- [4] M. W. Shafer, R. MacCurdy, J. R. Shipley, D. Winkler, C. G. Guglielmo, and E. Garcia, "The case for energy harvesting on wildlife in flight," *Smart Materials and Structures*, vol. 24, no. 2, p. 025031, 2015.
- [5] M. Han, H. Wang, Y. Yang, C. Liang, W. Bai, Z. Yan, H. Li, Y. Xue, X. Wang, B. Akar *et al.*, "Three-dimensional piezoelectric polymer microsystems for vibrational energy harvesting, robotic interfaces and biomedical implants," *Nature Electronics*, vol. 2, no. 1, pp. 26–35, 2019.
- [6] M. R. Sarker, S. Julai, M. F. M. Sabri, S. M. Said, M. M. Islam, and M. Tahir, "Review of piezoelectric energy harvesting system and application of optimization techniques to enhance the performance of the harvesting system," *Sensors and Actuators A: Physical*, vol. 300, p. 111634, 2019.
- [7] M. P. Bendsoe and O. Sigmund, *Topology Optimization: Theory, Methods and Applications*. Springer, Feb. 2004.
- [8] —, *Topology Optimization Theory, Methods and Applications*. Springer Science & Business Media, 2003.
- [9] M. P. Bendsoe and N. Kikuchi, "Generating optimal topologies in structural design using a homogenization method," 1988.
- [10] C. J. Rupp, A. Evgrafov, K. Maute, and M. L. Dunn, "Optimal design of piezoelectric energy harvesters based on multilayer plates and shells," in *Smart Materials, Adaptive Structures and Intelligent Systems*, vol. 43314, 2008, pp. 509–515.
- [11] —, "Design of piezoelectric energy harvesting systems: a topology optimization approach based on multilayer plates and shells," *Journal of Intelligent Material Systems and Structures*, vol. 20, no. 16, pp. 1923–1939, 2009.
- [12] B. Zheng, C.-J. Chang, and H. C. Gea, "Topology optimization of energy harvesting devices using piezoelectric materials," *Structural and Multidisciplinary Optimization*, vol. 38, no. 1, pp. 17–23, 2009.
- [13] J. Y. Noh and G. H. Yoon, "Topology optimization of piezoelectric energy harvesting devices considering static and harmonic dynamic loads," *Advances in Engineering Software*, vol. 53, pp. 45–60, 2012.
- [14] M. Kögl and E. C. Silva, "Topology optimization of smart structures: design of piezoelectric plate and shell actuators," *Smart materials and Structures*, vol. 14, no. 2, p. 387, 2005.
- [15] R. Salas, F. Ramírez, W. Montealegre-Rubio, E. Silva, and J. Reddy, "A topology optimization formulation for transient design of multi-entry laminated piezocomposite energy harvesting devices coupled with electrical circuit," *International Journal for Numerical Methods in Engineering*, vol. 113, no. 8, pp. 1370–1410, 2018.
- [16] T. Schlinquer, A. Homayouni-Amlashi, M. Rakotondrabe, and A. M. Ousaid, "Design of piezoelectric actuators by optimizing the electrodes topology," *IEEE Robotics and Automation Letters*, vol. 6, no. 1, pp. 72–79, 2020.
- [17] B. Yang, C. Cheng, X. Wang, Z. Meng, and A. Homayouni-Amlashi, "Reliability-based topology optimization of piezoelectric smart structures with voltage uncertainty," *Journal of Intelligent Material Systems and Structures*, vol. 33, no. 15, pp. 1975–1989, 2022.
- [18] T. Schlinquer, A. Mohand-Ousaid, and M. Rakotondrabe, "Displacement amplifier mechanism for piezoelectric actuators design using simple topology optimization approach," in *IEEE ICRA*, 2018, pp. 1–7.
- [19] A. Homayouni, A. Mohand Ousaid, and M. Rakotondrabe, "Topology optimization of piezoelectric plate energy harvester under external in-plan force considering different boundary conditions," in *2019 International Conference on Manipulation, Automation and Robotics at Small Scales (MARSS 2019)*, Helsinki, Finland, jul 2019, pp. 1 – 6. [Online]. Available: <https://publiweb.femto-st.fr/tntnet/entries/15824/documents/author/data>
- [20] A. Homayouni-Amlashi, A. Mohand-Ousaid, and M. Rakotondrabe, "Topology optimization of 2dof piezoelectric plate energy harvester under external in-plane force," *Journal of Micro-Bio Robotics*, pp. 1–13, 2020.
- [21] A. Homayouni-Amlashi, A. M. Ousaid, and M. Rakotondrabe, "Multi directional piezoelectric plate energy harvesters designed by topology optimization algorithm," *IEEE Robotics and Automation Letters*, 2019.
- [22] A. Homayouni-Amlashi, T. Schlinquer, A. Mohand-Ousaid, and M. Rakotondrabe, "2d topology optimization matlab codes for piezoelectric actuators and energy harvesters," *Structural and Multidisciplinary Optimization*, pp. 1–32, 2020.
- [23] S.-G. Kim, S. Priya, and I. Kanno, "Piezoelectric mems for energy harvesting," 2012.
- [24] A. Erturk and D. J. Inman, *Piezoelectric energy harvesting*. John Wiley Sons, 2011.
- [25] C. Kim and J.-W. Shin, "Topology optimization of piezoelectric materials and application to the cantilever beams for vibration energy harvesting," *International Journal of Precision Engineering and Manufacturing*, vol. 14, no. 11, pp. 1925–1931, 2013.
- [26] X. Wang, Z. Lin, and Y. Ren, "Topology optimization of piezocomposite resonator for maximizing excitation strength and synthesizing desired eigenmodes," *Acta Mechanica Solida Sinica*, vol. 30, no. 5, pp. 531–539, 2017.
- [27] K. Rabenorosoa and M. Rakotondrabe, "Performances analysis of piezoelectric cantilever based energy harvester devoted to mesoscale intra-body robot," *SPIE Sensing Technology+Applications*, 2015.
- [28] R. Lerch, "Simulation of piezoelectric devices by two-and three-dimensional finite elements," *IEEE transactions on ultrasonics, ferroelectrics, and frequency control*, vol. 37, no. 3, pp. 233–247, 1990.
- [29] X. Huang, Z. Zuo, and Y. Xie, "Evolutionary topological optimization of vibrating continuum structures for natural frequencies," *Computers & structures*, vol. 88, no. 5-6, pp. 357–364, 2010.
- [30] N. L. Pedersen, "Maximization of eigenvalues using topology optimization," *Structural and multidisciplinary optimization*, vol. 20, no. 1, pp. 2–11, 2000.
- [31] K. Svanberg, "The method of moving asymptotes—a new method for structural optimization," *International journal for numerical methods in engineering*, vol. 24, no. 2, pp. 359–373, 1987.
- [32] —, "Mma and gmma-two methods for nonlinear optimization," *vol*, vol. 1, pp. 1–15, 2007.
- [33] A. Donoso, E. Aranda, and D. Ruiz, "A new method for designing piezo transducers with connected two-phase electrode," *Computers & Structures*, vol. 275, p. 106936, 2023.
- [34] A. Donoso and J. K. Guest, "Topology optimization of piezo modal transducers considering electrode connectivity constraints," *Computer Methods in Applied Mechanics and Engineering*, vol. 356, pp. 101–115, 2019.
- [35] J.-H. Park, H.-Y. Bae, Y.-R. Oh, Y.-J. Kim, H. Kim, and Y.-H. Huh, "Tensile test of lead zirconate titanate (pzt)/platinum (pt) thin film," *Materialwissenschaft und Werkstofftechnik*, vol. 42, no. 5, pp. 478–484, 2011.